JOC Articles

Density Functional Theory Studies of Negishi Alkyl–Alkyl Cross-Coupling Reactions Catalyzed by a Methylterpyridyl-Ni(I) Complex

Xufeng Lin and David Lee Phillips*

Department of Chemistry, The University of Hong Kong, Pokfulam Road, Hong Kong 11111, People's Republic of China

phillips@hkucc.hku.hk

Received May 15, 2007

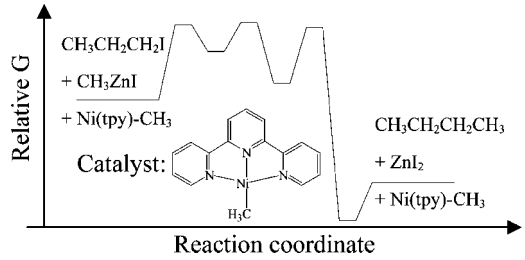

Density functional theory calculations were done to examine the potential energy surfaces of Ni(I)-catalyzed Negishi alkyl–alkyl cross-coupling reactions by using propyl iodide and isopropyl iodide as model alkyl electrophiles and CH_3ZnI as a model alkyl nucleophile. A four-step catalytic cycle involving iodine transfer, radical addition, reductive elimination, and transmetalation steps were characterized structurally and energetically. The reaction mechanism for this catalytic cycle appears feasible based on the calculated free energy profiles for the reactions. The iodine transfer step is the rate-determining step for the Ni(tpy)-CH_3 (tpy = 2,2′6′,2″-terpyridine) reactions with alkyl iodides. For secondary alkyl electrophiles, the oxidative addition intermediate, Ni(III), prefers to undergo decomposition over reductive elimination, whereas for the primary alkyl electrophiles, Ni(III) prefers to undergo reductive elimination over decomposition based on comparison of the relative reaction rates for these two types of steps. In addition, thermodynamic data were employed to help explain why the yield of the coupled product is very low from the Ni(II)-alkyl halide reactions with organozinc reagents.

1. Introduction

C−C bond formation reactions are one of the most important transformations in synthetic chemistry because they provide many ways to build up complex structures from readily available reagents. The C−C cross-coupling of a C−X bond (where X = Cl, Br, I, OTf, OMs, N_2^+, etc. and the reactant containing this bond is an alkyl electrophile) with a C−Y bond (where Y = ZnX, MgX, BX_2, etc. and the reactant containing this bond is an alkyl nucleophile) has been achieved using catalysis reactions involving nickel or palladium complexes.[1,2] These catalytic reactions are generally believed to involve oxidative addition, transmetalation, and reductive elimination steps as indicated in Scheme 1.[2d] However, a number of obstacles have made the application of these kinds of catalytic reactions difficult for $C(sp^3)-C(sp^3)$ bond formation. For example, the undesired side reaction of β-H elimination of the oxidative addition intermediate can take place in some cases (see the right part of Scheme 1). Furthermore, common alkyl electrophiles are well-known to oxidize low-valence transition metals by single-electron processes and lead to formation of alkyl radicals. Possible side reactions of alkyl radicals (such as dimerization reactions) instead of radical attack on the transition metal can

(1) (a) Diederich, F., Stang, P. J. *Metal-Catalyzed Cross-Coupling Reactions*; Wiley-VCH: Weinheim, Germany, 1998. (b) de Meijere, A.; Diederich, F. *Metal-Catalyzed Cross-Coupling Reactions*, 2nd ed.; Wiley-VCH: Weinheim, Germany, 2004. (c) Beller, M.; Bolm, C. *Transition Metals for Organic Synthesis*, 2nd ed., Wiley-VCH: Weinheim, 2004.

10.1021/jo702497p CCC: $40.75
Published on Web 04/15/2008

lead to inefficient catalysis of the desired cross-coupling reactions. The pioneering work of a number of groups including Kochi and Tamura,[3] Suzuki and co-workers,[4] and Knochel and co-workers[5] have demonstrated the general feasibility of metal-catalyzed cross-coupling reactions with nonactivated primary alkyl electrophiles. In recent years, a great deal of progress has been made in identifying ligands and reaction conditions that effectively promote alkyl–alkyl cross-coupling reactions for a variety of applications.[6–10] An important contribution has been made by Fu and co-workers[8,9] in developing cross-coupling reactions with unactivated secondary alkyl electrophiles.[9] They found that efficient Ni-catalyzed secondary electrophiles such as benzylic halides or α-bromo amides could react with an organozinc reagent (RZnX) so that Negishi-type reactions could be achieved by using the pybox (pybox = bis(oxazolinyl)pyridine) ligand. Reaction conditions were then found to exploit the C_2 symmetry of the modified pybox ligands, and racemic alkyl electrohpiles could be converted into enantioselective products with an *ee* value up to 92%.[9]

However, mechanistic work for these types of catalytic reactions[6–10] is still elusive in the literature. Several experimental results tend not to support the traditional reaction mechanisms depicted in Scheme 1 and some new mechanisms have been proposed. For example, Kambe and co-workers[6a] proposed a mechanism that involves bis-π-allyl nickel complex [Ni(II)] catalyzed cross-coupling reactions of Grignard reagents with alkyl electrophiles. In this mechanism, the Ni(II) catalyst first undergoes transmetalation with the Grignard reagent and then is followed by an oxidative addition of an alkyl halide to give a Ni(IV) intermediate. Reductive elimination of this intermediate yields the coupled product and regenerates the active Ni(II) catalyst. Recently, Vivic and co-workers have reported a series of Ni-catalyzed Negishi alkyl–alkyl cross-coupling reactions

SCHEME 1. Postulated Reaction Mechanisms for the Alkyl−Alkyl Cross-Coupling Reaction and the β-H Elimination Side Reaction[a]

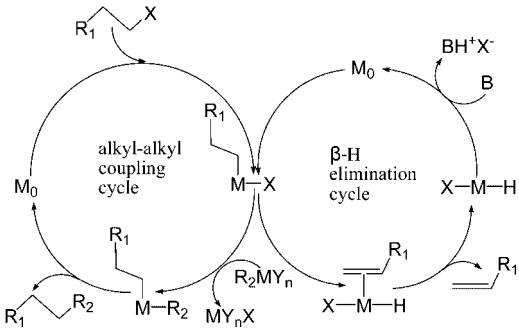

[a] Reproduced from a scheme shown in ref 2d.

SCHEME 2. Reaction Mechanism Proposed in Scheme 3 in Reference 10c

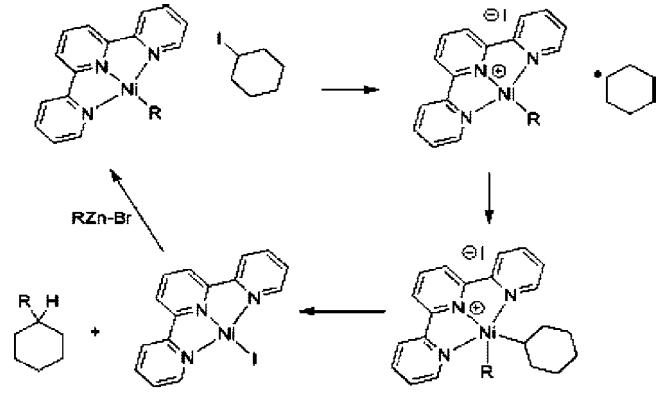

with several pyridine based tridentate-nitrogen ligands.[10b,c] They reported that a methylterpyridylnickel iodide [a Ni(II) complex] reacts with a transmetalating organozinc reagent with a yield of only 8%. This evidence is not consistent with the general catalytic cycle shown in Scheme 1 in which Ni(0) oxidatively adds an alkyl halide and subsequently undergoes a simple transmetalation reaction to produce the cross-coupling product. Reaction of terpyridine with (TMEDA)Ni(CH_3)$_2$ (TMEDA = *N*,*N*′,*N*′-tetramethylethylenediamine) produces a monomethylterpyridyl Ni(I) complex, (denoted as Ni(tpy)-CH_3, where tpy = 2,2′6′,2″-terpyridine), instead of a dimethyl complex. Ni(tpy)-CH_3 was found to effectively transfer its methyl group to alkyl iodides to form cross-coupled alkanes with high yields. Based on these results, a new mechanism was proposed that employs a Ni(I) complex as the key catalyst (see Scheme 2). In this mechanism, the alkyl halide oxidatively transfers the halogen atom to the Ni(tpy)-CH_3 species to produce a Ni(II) complex and an alkyl radical. This is then followed by an alkyl radical attack on the Ni atom to produce a Ni(III) complex. Reductive elimination of this Ni(III) complex produces the coupled product and a Ni(tpy)-I species that reacts with the organozinc reagent to recycle the catalyst. Unfortunately, no kinetics study or computational characterization of this proposed reaction mechanism appears to have been done to verify such a catalytic cycle.

To gain a deeper insight into the chemistry of these kinds of metal-catalyzed C−C bond formation reactions, we have employed computational tools to explore the potential energy surfaces of Ni-catalyzed Negishi alkyl–alkyl cross-coupling reactions. Our computations found that the traditional mechanism depicted in Scheme 1 appears not to be easy to take place for the model reaction systems. Our study also examined the

(2) (a) Cardenas, D. J. *Angew. Chem., Int. Ed.* **1999**, *38*, 3018–3020. (b) Luh, T. Y.; Leung, M. K.; Wong, K. T. *Chem. Rev.* **2000**, *100*, 3187–3204. (c) Cardenas, D. J. *Angew. Chem., Int. Ed.* **2003**, *42*, 384–387. (d) Frisch, A. C.; Beller, M. *Angew. Chem., Int. Ed.* **2005**, *44*, 674–688.

(3) (a) Kochi, J. K.; Tamura, M. *J. Am. Chem. Soc.* **1971**, *93*, 1483–1485. (b) Kochi, J. K.; Tamura, M. *J. Am. Chem. Soc.* **1971**, *93*, 1485–1487. (c) Tamura, M.; Kochi, J. K. *J. Organomet. Chem.* **1972**, *42*, 205–228.

(4) (a) Ishiyama, T.; Abe, S.; Miyaura, N.; Suzuki, A. *Chem. Lett.* **1992**, 691–694. (b) Miyaura, N.; Suzuki, A. *Chem. Rev.* **1995**, *95*, 2457–2483. (c) Suzuki, A. *J. Organomet. Chem.* **1999**, *576*, 147–168.

(5) (a) Devasagayaraj, A.; Stüdemann, T.; Knochel, P. *Angew. Chem., Int. Ed. Engl.* **1995**, *34*, 2723–2725. (b) Giovannini, R.; Stuedemann, T.; Devasagayaraj, A.; Dussin, G.; Knochel, P. *J. Org. Chem.* **1999**, *64*, 3544–3553. (c) Giovannini, R.; Studemann, T.; Dussin, G.; Knochel, P. *Angew. Chem., Int. Ed.* **1998**, *37*, 2387–2390. (d) Jensen, A. E.; Knochel, P. *J. Org. Chem.* **2002**, *67*, 79–85.

(6) (a) Terao, J.; Watanabe, H.; Ikumi, A.; Kuniyasu, H.; Kambe, N. *J. Am. Chem. Soc.* **2002**, *124*, 4222–4223. (b) Terao, J.; Todo, H.; Watanabe, H.; Ikumi, A.; Kambe, N. *Angew. Chem., Int. Ed.* **2004**, *43*, 6180–6182.

(7) (a) Hadei, N.; Kantchev, E. A. B.; O'Brien, C. J.; Organ, M. G. *Org. Lett.* **2005**, *7*, 3805–3807. (b) Hadei, N.; Kantchev, E. A. B.; O'Brien, C. J.; Organ, M. G. *J. Org. Chem.* **2005**, *70*, 8503–8507.

(8) (a) Netherton, M. R.; Dai, C.; Neuschüz, K.; Fu, G. C. *J. Am. Chem. Soc.* **2001**, *123*, 10099–10100. (b) Kirchhoff, J. H.; Dai, C.; Fu, G. C. *Angew. Chem., Int. Ed.* **2002**, *41*, 1945–1947. (c) Netherton, M. R.; Fu, G. C. *Angew. Chem., Int. Ed.* **2002**, *41*, 3910–3912. (d) Tang, H. F.; Menzel, K.; Fu, G. C. *Angew. Chem., Int. Ed.* **2003**, *41*, 5079–5082. (e) Wiskur, S. L.; Korte, A.; Fu, G. C. *J. Am. Chem. Soc.* **2004**, *126*, 82–83.

(9) (a) Zhou, J.; Fu, G. C. *J. Am. Chem. Soc.* **2003**, *125*, 14726–14727. (b) Powell, D. A.; Fu, G. C. *J. Am. Chem. Soc.* **2004**, *126*, 7788–7789. (c) Zhou, J.; Fu, G. C. *J. Am. Chem. Soc.* **2004**, *126*, 1340–1341. (d) Arp, F. O.; Fu, G. C. *J. Am. Chem. Soc.* **2005**, *127*, 10482–10483. (e) Fischer, C.; Fu, G. C. *J. Am. Chem. Soc.* **2005**, *127*, 4594–4595. (f) González-Bobes, F.; Fu, G. C. *J. Am. Chem. Soc.* **2006**, *128*, 5360–5361.

(10) (a) Anderson, T. J.; Jones, G. D.; Vicic, D. A. *J. Am. Chem. Soc.* **2004**, *126*, 8100–8001. [erratum p 11113]. (b) Jones, G. D.; McFarland, C.; Anderson, T. J.; Vicic, D. A. *Chem. Commun.* **2005**, 4211–4213. (c) Jones, G. D.; Martin, J. L.; McFarland, C.; Allen, O. R.; Hall, R. E.; Haley, A. D.; Brandon, R. J.; Konovalova, T.; Desrochers, P. J.; Pulay, P.; Vicic, D. A. *J. Am. Chem. Soc.* **2006**, *128*, 13175–13183.

model reaction systems to characterize the reaction steps involved in the reaction mechanism depicted in Scheme 2 and to determine if this mechanism occurs more easily than the traditional mechanism in terms of their free energy profiles. Catalytic cycles with primary and secondary alkyl electrophiles were compared for both types of reaction mechanisms investigated here.

2. Computational Details

Propyl and isopropyl iodides were used to represent primary and secondary alkyl halides (R^1-X, R^1 = propyl, isopropyl, X = I) respectively in our model calculations. Methylzinc iodide (CH_3ZnI) was used to model the transmetalating reagent in the model computations. 2,2′,6′,2″-terpyridine (denoted as tpy in this paper) was used to model the trinitrogen ligands employed in the experimental work of Vicic and co-workers[10] and Fu and co-workers.[9] Density functional theory calculations were performed using the B3LYP[11] exchange and correlation functionals to explore the potential energy surfaces (PES) of the model Ni-catalyzed Negishi alkyl–alkyl cross-coupling reactions. The 6–31G* basis set was used for all C, H, O, N, Ni, and Zn atoms, and the LANL2DZ basis set in conjunction with an additional *d* polarization[12] of 0.266 was used for the I atoms. Five component *d* functions were employed in the calculations. This overall basis set is denoted as BS1 in this paper. The structure of Ni(tpy′)-CH_3 (tpy′ = 4,4′,4″-tri-*tert*-butylterpyridine) was optimized at the B3LYP/6–31G* level of theory, and the geometrical parameters obtained were found to be close to those from a X-ray experimental structure reported in ref 10c (see comparison in Figure 1S in the Supporting Information). The errors of the predicted bond lengths and bond angles compared to the experimental data are within ± 1.2%. This indicates the B3LYP/BS1 calculations provide a reasonable description of the systems we plan to study.

The PES for the reactions of interest were explored by optimizing geometries in the energy minimums for the reactants, the intermediates, and the products and the first-order saddle points for transition states using the Gaussian 98 program suite (employing the A.11 version of the programs).[13] Natural bond orbital analyses (NBO) were performed for the charge distributions of the calculated structures. Vibrational analyses were performed to confirm energy minimums and first-order saddle points as well as to obtain the zero-point corrected energies (ZPE) and free energies (at 298.15 K) of the optimized geometries. The polarized continuum model (PCM)[14] (implemented in the Gaussian 03 C.02 version of the program) was used to take into account the solvation effects of the THF ($\epsilon = 7.58$) solvent used in the experiments reported in ref 10. Cartesian coordinates, the total energies, and selected output from the calculations for all of the calculated structures are provided in the Supporting Information. Intrinsic reaction coordinate (IRC) computations were done to confirm the transition states connected the appropriate reactants and products.[15]

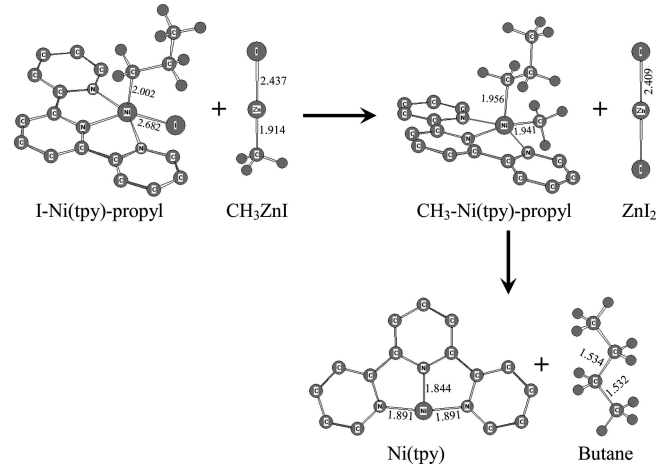

FIGURE 1. Optimized geometries obtained from B3LYP/BS1 calculations of the species involved in reaction Z. Hydrogen atoms in the terpyridine ring and in tert-butyl groups were deleted for clarity in this and subsequent figures in this paper. Selected key distances (in Å) are indicated.

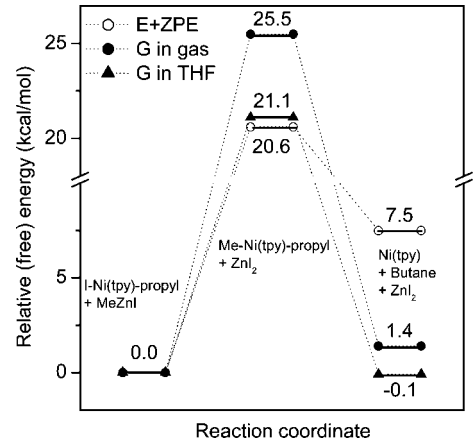

FIGURE 2. Schematic diagram of the energy and free energy profiles for eqs 1 and 2 in the gas phase and in the solution phase (THF).

3. Results and Discussion

3.1. The Reaction of I−Ni(tpy)-$CH_2CH_2CH_3$ with CH_3ZnI. Vivic and co-workers reported that the Ni(II)-alkyl halide did not react appreciably with an excess transmetalation agent to produce the cross-coupling product.[10b,c] For the modeling reaction of I−Ni(tpy)-propyl with CH_3ZnI, the transmetalation and reductive elimination steps can be written as follows:

$$\text{I}-\text{Ni(tpy)}-\text{CH}_2\text{CH}_2\text{CH}_3 + \text{CH}_3\text{ZnI} \rightarrow \text{CH}_3\text{-Ni(tpy)}-\text{CH}_2\text{CH}_2\text{CH}_3 + \text{ZnI}_2 \quad (1)$$

$$\text{CH}_3-\text{Ni(tpy)}-\text{CH}_2\text{CH}_2\text{CH}_3 \rightarrow \text{Ni(tpy)} + \text{CH}_3\text{CH}_2\text{CH}_2\text{CH}_3 \quad (2)$$

with the overall reaction of

(11) (a) Parr, R. G.; Yang, W. *Density Functional Theory of Atoms and Molecules*; Oxford: New York, 1989. (b) Ziegler, T. *Chem. Rev.* **1991**, *91*, 651–667. (c) Lee, C.; Yang, W.; Parr, R. G. *Phys. Rev. B* **1988**, *37*, 785–789. (d) Becke, A. D. *Phys. Rev. A* **1988**, *38*, 3098–3100.

(12) Huzinaga, S.; Anzelm, J.; Klobukowski, M.; Radzio-Andzelm, E.; Sakai, Y.; Tatewaki, H. In *Gaussian Basis Sets for Molecular Calculations*; Elsevier: Amsterdam, 1984.

(13) Frisch, M. J.; Trucks, G. W.; Schlegel, H. B.; Scuseria, G. E.; Robb, M. A.; Cheeseman, J. R.; Zakrzewski, V. G.; Montgomery, Jr., J. A.; Stratmann, R. E.; Burant, J. C.; Dapprich, S.; Millam, J. M.; Daniels, A. D.; Kudin, K. N.; Strain, M. C.; Farkas, O.; Tomasi, J.; Barone, V.; Cossi, M.; Cammi, R.; Mennucci, B.; Pomelli, C.; Adamo, C.; Clifford, S.; Ochterski, J.; Petersson, G. A.; Ayala, P. Y.; Cui, Q.; Morokuma, K.; Rega, N.; Salvador, P.; Dannenberg, J. J.; Malick, D. K.; Rabuck, A. D.; Raghavachari, K.; Foresman, J. B.; Cioslowski, J.; Ortiz, J. V.; Baboul, A. G.; Stefanov, B. B.; Liu, G.; Liashenko, A.; Piskorz, P.; Komaromi, I.; Gomperts, R.; Martin, R. L.; Fox, D. J.; Keith, T.; Al-Laham, M. A.; Peng, C. Y.; Nanayakkara, A.; Challacombe, M.; Gill, P. M. W.; Johnson, B.; Chen, W.; Wong, M. W.; Andres, J. L.; Gonzalez, C.; Head-Gordon, M.; Replogle, E. S.; Pople, J. A. *Gaussian 98*, revision A.11; Gaussian, Inc.: Pittsburgh, 2002.

(14) (a) Miertus, S.; Scrocco, E.; Tomasi, J. *J. Chem. Phys.* **1981**, *55*, 117–129. (b) Miertus, S.; Tomasi, J. *Chem. Phys.* **1982**, *65*, 239–245. (c) Cossi, M.; Barone, V.; Cammi, R.; Tomasi, J. *Chem. Phys. Lett.* **1996**, *255*, 327–335.

(15) (a) Gonzalez, C.; Schlegel, H. B. *J. Chem. Phys.* **1989**, *90*, 2154–2161. (b) Gonzalez, C.; Schlegel, H. B. *J. Phys. Chem.* **1990**, *94*, 5523–5527.

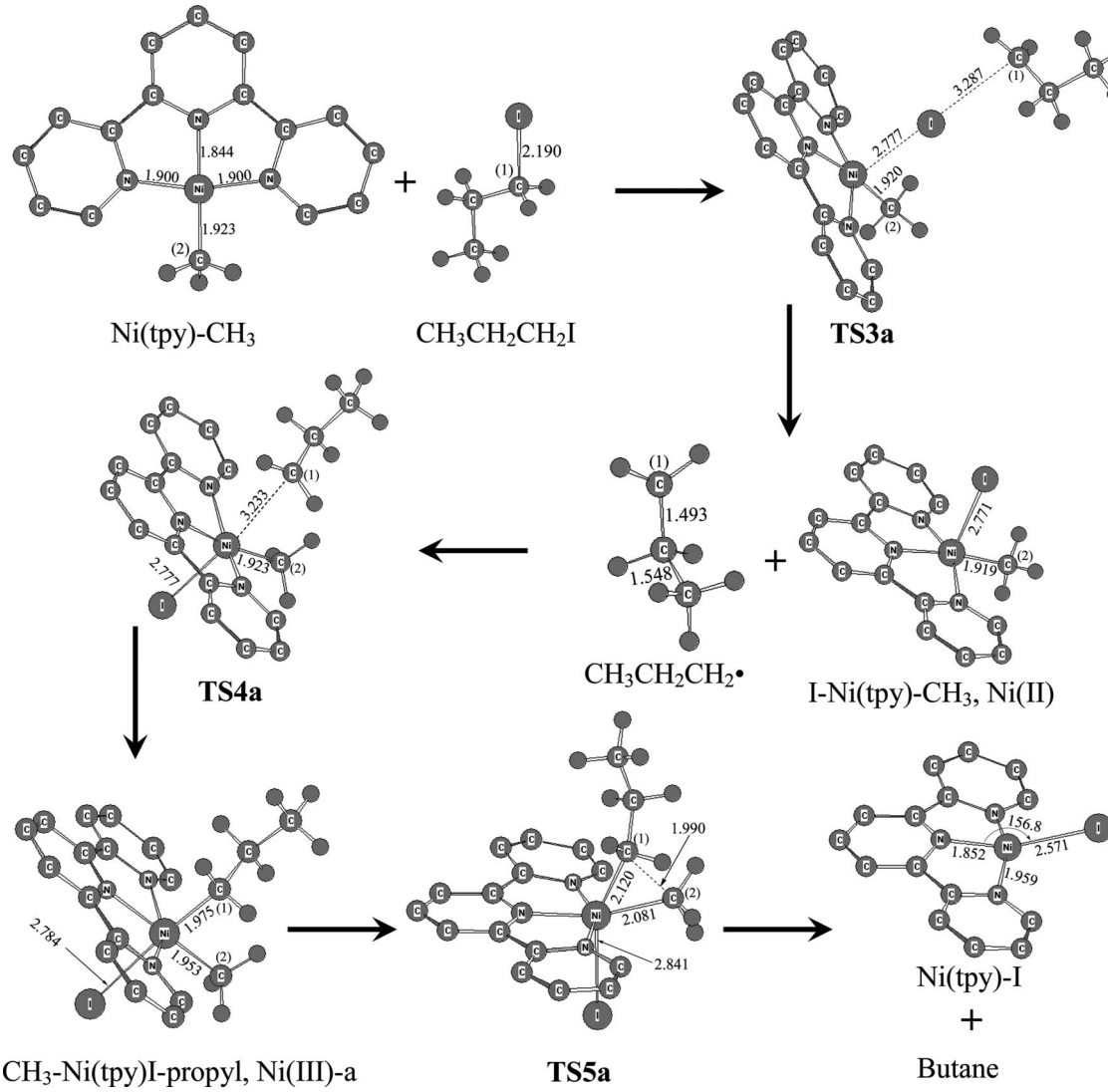

FIGURE 3. Optimized geometries in B3LYP/BS1 level for the reactants, the transition states intermediates, and the products involved in the reaction of eqs 3a−5a. Key bond lengths (in Å) are indicated.

$$\mathrm{Ni(tpy)-CH_2CH_2CH_3 + CH_3ZnI \rightarrow Ni(tpy) + CH_3CH_2CH_2CH_3 + ZnI_2} \quad (Z)$$

The optimized geometries of the species involved in reaction Z are presented in Figure 1, and the thermodynamic data of these species in the gas phase and in THF solution are depicted in Figure 2. We did not find the transition state for eq 1 in spite of several attempts, whereas upon inspection of Figure 2, reaction Z is not thermodynamically favorable. The energy and the free energy profiles depicted in Figure 2 show that eq 1 is endothermic with an energy increase of 20.6 kcal/mol and is highly unfavorable with a free energy increase of 25.5 kcal/mol. Although the reductive elimination (eq 2) of the transmetalation product is favored by an energy decrease of 13.1 kcal/mol and a free energy decrease of 24.1 kcal/mol, the overall free energy change for reaction Z is still slightly disfavored by an overall free energy increase of 1.4 kcal/mol. Considering the solvation effect by PCM calculations, we found that the CH_3-Ni(tpy)-propyl species is still largely disfavored by a free energy increase of 21.1 kcal/mol and the overall free energy change for reaction Z is very close to 0 kcal/mol. In a word, it is largely disfavored in the generation of the transmetalation product (e.g., CH_3-Ni(tpy)-propyl in eq 1) and the subsequent reductive elimination step (eq 2) does not provide enough free energy compensation to effectively drive eq 1 to the "right direction". The above results suggest that the mechanism in which the oxidative addition product of Ni(II) reacts to form a transmetalating reagent and then followed by a reductive elimination (see Scheme 1) is not feasible for Ni-catalyzed alkyl–alkyl cross-coupling reactions with the ligand of terpyridine, which is consistent with the result reported in ref 10c.

3.2. Reaction of Ni(tpy)−CH_3 with Propyl Iodide. In the literature, there are several reports on the computational characterizations and a concerted pathway was believed to be operate for alkenyl or aryl halides oxidatively added to Pd[16]

(16) (a) Ahlquist, M.; Norrby, P. O. *Organometallics* **2007**, *26*, 550–553. (b) Álvarez, R.; Faza, O. N.; de Lera, A. R.; Cárdenas, D. J. *Adv. Synth. Catal.* **2007**, *349*, 887–906. (c) Braga, A. A. C.; Ujaque, G.; Maseras, F. *Organometallics* **2006**, *25*, 3647–3658. (d) Goossen, L. J.; Koley, D.; Hermann, H. L.; Thiel, W. *Organometallics* **2006**, *25*, 54–67. (e) Álvarez, R.; Faza, O. N.; López, C. S.; de Lera, Á. R. *Org. Lett.* **2006**, *8*, 35–38. (f) Braga, A. A. C.; Morgon, N. H.; Ujaque, G.; Maseras, F. *J. Am. Chem. Soc.* **2005**, *127*, 9298–9307. (g) Goossen, L. J.; Koley, D.; Hermann, H. L.; Thiel, W. *J. Am. Chem. Soc.* **2005**, *127*, 11102–11114. (h) Ma, S.; Ren, H.; Wei, Q. *J. Am. Chem. Soc.* **2003**, *125*, 4817–4830.

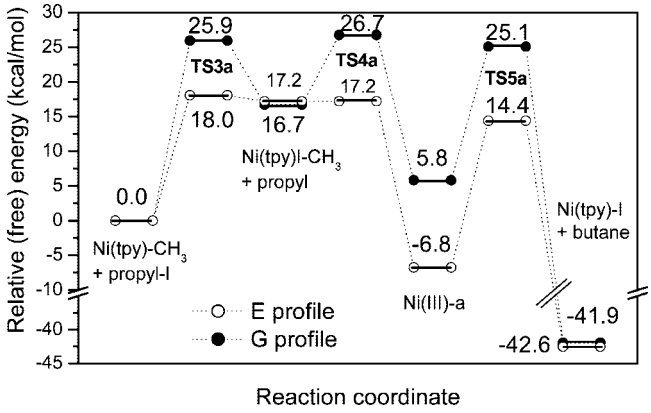

FIGURE 4. Schematic diagram of the energy (○) and the free energy (●) profiles for the reactions of 3a−5a. See text and Figure 3 for details.

and Ni.[16h] However, compared to alkenyl or aryl halides, alkyl halides are more electron rich, which lead to lower propensity in addition to a metal center.[2d] Common alkyl electrophiles typically oxidize low-valence transition metals by single-electron processes.[9d,f,10a,c,17] For Ni(tpy)−CH_3 reacting with alkyl halide, Vicic et al. believed the presence of radical pathway after checking the minor product.[10a] They have proposed two mechanistic schemes containing a radical pathway.[10a,c] Furthermore, the result of Fu's works[9d,f] shows that in the Ni-catalyzed cross-coupling reactions, racemic secondary alkyl halides can be converted to a high enantioselective coupled products. This suggests there is a stereoconvergence process, i.e., a radical pathway, since a concerted pathway leads to chiralty-retention products. In this work, the oxidative addition of an alkyl halide to the Ni(I) species via a radical pathway were examined in two reaction steps (using our model compounds) as shown below in eqs 3a and 4a. There are two alkyl groups connected to the metal center produced in the Ni(III) product of eq 4a. This Ni(III) species undergoes reductive elimination as shown in eq 5a to form the alkyl–alkyl coupled product and another Ni(I) species, Ni(tpy)−I.

$$\mathrm{Ni(tpy)-CH_3 + CH_3CH_2CH_2I \rightarrow I-Ni(tpy)-CH_3 + CH_3CH_2CH_2^{\cdot}} \quad (3a)$$

$$\mathrm{I-Ni(tpy)-CH_3 + CH_3CH_2CH_2^{\cdot} \rightarrow CH_3-Ni(tpy)I-CH_2CH_2CH_3} \quad (4a)$$

$$\mathrm{CH_3-Ni(tpy)I-CH_2CH_2CH_3 \rightarrow Ni(tpy)I + CH_3CH_2CH_2CH_3} \quad (5a)$$

The overall reaction equation is:

$$\mathrm{Ni(tpy)-CH_3 + CH_3CH_2CH_2CH_3I \rightarrow Ni(tpy)-I + CH_3CH_2CH_2CH_3} \quad (A)$$

The geometries optimized at the B3LYP/BS1 level of theory for the reactants, the transition states, the intermediates and the products involved in reaction A are displayed in Figure 3. The energy and free energy profiles for this reaction are presented in Figure 4. The Ni(tpy)−CH_3 species has a planar structure, and the propyl iodide attacks the Ni atom on one side of the tpy plane with the Ni, I, and $C^{(1)}$ atoms roughly in a line in the transition state structure of eq 3a. The I atom is detached from the $C^{(1)}$ atom with an I···$C^{(1)}$ distance of 3.287 Å and approaches the Ni atom with a I···Ni distance of 2.777 Å in **TS3a**. The imaginary frequency of **TS3a** indicates a clear I atom movement between Ni and $C^{(1)}$ atoms. The I···Ni distance is very close to that (2.771 Å) found in the Ni(II) product, I−Ni(tpy)−CH_3, and this indicates that the I atom transfer has a "late" transition state. We note the caveat that the potential energy surface in the **TS3a** and **TS4a** regions is fairly flat and these transition states have low imaginary frequencies so that their physical meaning is not entirely unambiguous. From the free energy profile shown in Figure 4, eq 3a is uphill in terms of energy by about 17 kcal/mol and has an energy of activation of 18.0 kcal/mol and a free energy of activation of 25.9 kcal/mol. To better evaluate the B3LYP/BS1 results on 3a, it was further characterized by computation at two higher basis set levels, denoted as BS2 and BS3, respectively. BS2 differs with BS1 only in that 6-311G** was used for I atom, and in BS3, 6-311G** was used for all C, H, N, and I atoms and 6-31G** was used for Ni atom. Table 1 lists the reaction barrier of eq 3a and selected geometric parameters of **TS3a**, and it can be seen that the results with B3LYP/BS2 and B3LYP/BS3 level of theory are rather close to that with B3LYP/BS1 level of theory.

The propyl radical attack on the Ni atom in the Ni(II) intermediate takes place on the other side of the tpy plane with respect to the I atom transfer step in the reaction of eq 3a. In the transition state, **TS4a**, the distance between the Ni atom

TABLE 1. Thermodynamic Data and Selected Geometrical Parameters Computed from Different Basis Set Level with B3LYP

basis set	BS1	BS2	BS3
$\Delta E_{3a}^{\ddagger}$ (kcal/mol)	19.2	17.8	19.3
$\Delta G_{3a}^{\ddagger}$ (kcal/mol)	25.9	26.0	27.3
Ni···I in **TS3a** (Å)	2.777	2.809	2.794
I···$C^{(1)}$ in **TS3a** (Å)	3.287	3.161	3.209

TABLE 2. Comparison of the Free Energy of Activation (in kcal/mol) of Each Steps Involved in Reactions *A* and *B*[a]

eq number	$\Delta G^{\ddagger}$ in gas phase	$\Delta G^{\ddagger}$ in THF solution
3a	25.9	22.2
4a	10.0	11.0
5a	19.3	18.9
−4a	20.9	21.4
3b	23.7	22.2
4b	13.2	13.6
5b	19.2	18.8
−4b	16.9	17.8

[a] Here eqs –4a and –4b are defined as the reverse reactions of eqs 4a and 4b.

TABLE 3. (Top) NBO Charge of Selected Atoms or Moieties of Equations *3a* and *4a* and (Bottom) Spin Densities of Selected Atoms or Moieties of Equation *3a*

species	Ni	TPY	$-C^{(2)}H_3$	I	propyl
Ni(tpy)-CH_3 + propyl-I	1.134	−0.591	−0.543	0.051	−0.051
TS3a	1.251	−0.171	−0.455	−0.635	0.009
I−Ni(tpy)-CH_3 +propyl	1.244	−0.094	−0.451	−0.699	0.000
TS4a	1.298	−0.101	−0.451	−0.689	−0.058
CH_3−Ni(tpy)I-propyl	1.407	0.077	−0.425	−0.683	−0.376

species	Ni	TPY	$-C^{(2)}H_3$	I	propyl	$C^{(1)}$
Ni(tpy)-CH_3 +propyl-I	0.073	0.930	−0.003	0.000	0.000	0.000
TS3a	−0.119	0.303	0.012	−0.102	0.906	0.984
I−Ni(tpy)-CH_3 +propyl	0.000	0.000	0.000	0.000	1.000	1.087

(17) (a) Weston, C. W.; Verstuyft, A. W.; Nelson, J. H.; Jonassen, H. B. *Inorg. Chem.* **1977**, *16*, 1313–1317. (b) Castano, A. M.; Echavarren, A. M. *Organometallics* **1994**, *13*, 2262–2268.

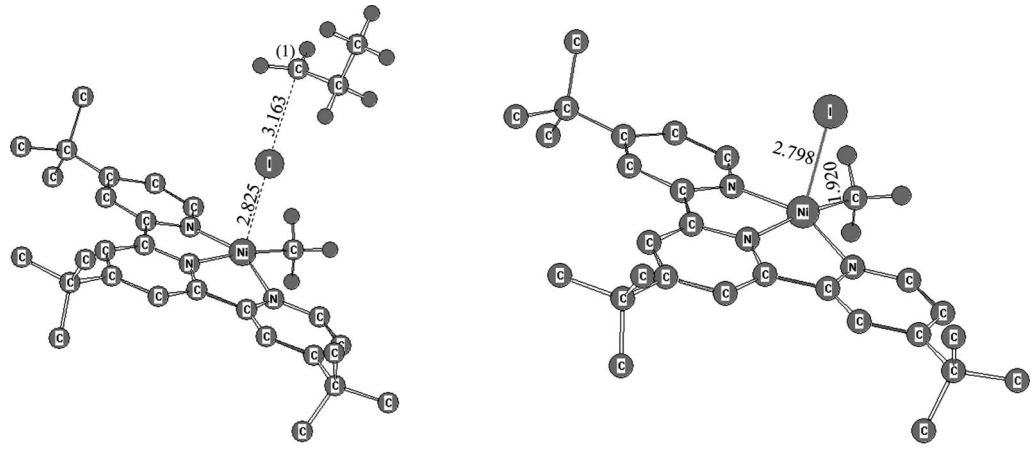

FIGURE 5. Selected B3LYP/BS1 optimized geometries of the transition state and products of the iodine atom transfer to the Ni(tpy′)−CH_3 complex involved in the process of Ni(tpy′)−CH_3 + $CH_3CH_2CH_2I$ → **TS3a′** → I−Ni(tpy′)−CH_3 + $CH_3CH_2CH_2^{\bullet}$.

and the incoming $C^{(1)}$ atom, is 3.233 Å. The energy of activation ($\Delta E_{4a}^{\ddagger}$) is nearly zero along the reaction coordinate in terms of the $C^{(1)}$ approach to the Ni atom while there is an overall free energy of activation of 10.0 kcal/mol for this process to produce the Ni(III) intermediate, CH_3−Ni(tpy)I-propyl (denoted as Ni(III)-a). This shows that the $\Delta G_{4a}^{\ddagger}$ originates mainly from the entropy of activation ($\Delta S^{\ddagger}$). The overall oxidative addition process (combination of eqs 3a and 4a) is slightly uphill in terms of the free energy and is exothermic by 6.8 kcal/mol in energy. For the reductive elimination step that starts from Ni(III)-a in 5a, a $C^{(1)}$−Ni−$C^{(2)}$ triangular structure can be identified in the transition state structure of **TS5a**, with a $C^{(1)}\cdots C^{(2)}$ distance of 1.990 Å. The approach of these two carbon atoms is accompanied by increases in the lengths of the two Ni−C bonds and one Ni−I bond upon going from Ni(III)-a to **TS5a**. It is interesting to note that each H atom connected to the $C^{(1)}$ and to $C^{(2)}$ atoms approach the Ni center with distances in the range of "agostic H"[18] distance of 1.8–2.3 Å. The "agostic" Ni−H interactions may help to lower the energy of the transition state. The products of the reaction of eq 5a are butane (see Figure 1) and another Ni(I) species (see Figure 3), Ni(tpy)−I. The free energy of activation for the reductive elimination step is 19.3 kcal/mol and the product of the reaction of eq 5a is highly exothermic with a free energy change of 47.7 kcal/mol.

The free energy of activation with incorporation of ΔG^{solv} in THF solution was listed in Table 2. The solvation effect leads to a lower free energy of activation for the reaction of eq 3a by 3.7 kcal/mol. The solvation effect lowers the free energies of the reactant [Ni(II) + propyl], the transition state (**TS4a**) and the product [Ni(III)] in eq 4a by 5.4, 4.4, and 4.9 kcal/mol, respectively; therefore, the radial-attack step has a 1.0 kcal/mol increase in free energy of activation. The reductive elimination step is also only slightly influenced by a 0.4 kcal/mol decrease in the free energy of activation. Table 2 shows both in gas-phase and solution-phase models, the I atom transfer step has the highest "reaction barrier" in reaction A. Taking into account that an alkyl electrophile is one of the starting materials in a common reaction system and is found in far larger amounts compared to the Ni compound(s), the reaction of 3a can be considered to be of first order in terms of consuming Ni(tpy)−CH_3. Although $\Delta G_{4a}^{\ddagger}$ is by far lower than $\Delta G_{3a}^{\ddagger}$, it should be noted that the concentration of the reactants for eq 4a [i.e., $CH_3CH_2CH_2^{\bullet}$ and the Ni(II) species] in the real reaction system may be low, because both of them are intermediates generated from the previous step (eq 3a). However, it is attractive to speculate that the I atom transfer from the alkyl iodide to the Ni(tpy)−CH_3 intermediate leaves an alkyl radical in close proximity to metal center[10c] and therefore the oxidative attack of the alkyl radical with the Ni(tpy)I-CH_3 intermediate may immediately be followed by the I atom transfer. Regarding that the Ni-catalyzed reaction undergoes in a solution phase, the solvent may help keep the product of 3a in close proximity by the so-called "solvent cage" effect.[19] This would make the reaction of 4a act more like a first-order reaction in terms of consuming the "Ni(tpy)I−$CH_3\cdots$propyl radical" pair. Equation 5a is a first-order reaction. So both in gas-phase and solution-phase models, the I atom transfer step is rate-determining in reaction A, whereas the absolute rate of the radical-attack step is an important factor for the final yield of cross-coupled product, since radicals are highly reactive intermediates.

Upon inspection of the NBO charge analysis listed in Table 3 (top) on reaction A, the iodine transfer step is accompanied by a noticeable charge transfer from the tpy ligand to the I atom. The charge of the I atom decreases (negative change) from 0.051 in propyl iodide to –0.635 in **TS3a**, while the charge of the propyl group only changes slightly. The charge of the Ni atom and the methyl group increase only by 0.117 and 0.088, respectively, while that of the tpy ligand increases by 0.420. This implies that the iodine atom adds to Ni atom by oxidizing the terpyridine ring rather than the Ni atom. For eq 4a, an increase of 0.163 in the charge of the Ni atom was found, which is accompanied by an increase of 0.171 in the charge of the tpy ligand and a decrease of 0.314 in the charge on the propyl group from comparison of the Ni(II) and Ni(III)-a structures. This shows that the propyl radical adds to the Ni atom by oxidizing the metal center and the tpy ring at the same time. To better

(18) Brookhart, M.; Green, M. L. H. *J. Organomet. Chem.* **1983**, *250*, 395–408.

(19) (a) Rabinowitch, E.; Wood, W. C. *Trans. Faraday Soc.* **1936**, *32*, 1381–1387. (b) Franck, J.; Rabinowitsch, E. *Trans. Faraday Soc.* **1934**, *30*, 120–131. (c) Rabinowitch, E. *Trans. Faraday Soc.* **1937**, *33*, 1225–1233. (d) Harris, J. D.; Oelkers, A. B.; Tyler, D. R. *J. Am. Chem. Soc.* **2007**, *129*, 6255–6262.

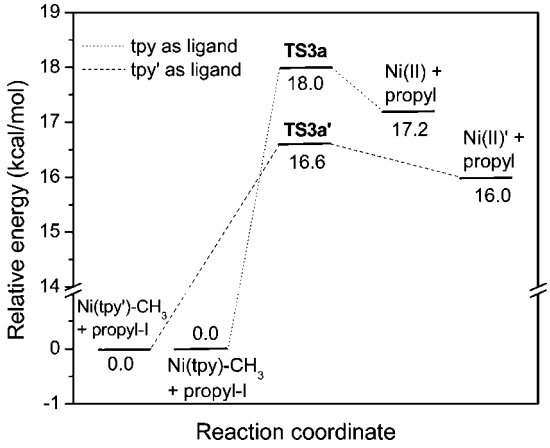

FIGURE 6. Comparison of the energy diagram of the iodine transfer processes for the propyl iodide reaction with Ni(tpy)−CH_3 and Ni(tpy′)−CH_3. See Figures 4 and 7 for details.

understand why the propyl iodide oxidizes the tpy ligand more than the Ni atom in the iodine atom transfer step, it is helpful to analyze the Kohn–Sham (KS) orbitals[20] of Ni(tpy)−CH_3. Upon examination of the molecular orbital coefficient and visualization of the selected molecular orbitals of Ni(tpy)−CH_3 (six selected visualized molecular orbitals are presented in Figure 2S in the Supporting Information), it was found that Ni 3d orbital contributes little to the singly occupied molecular orbital (SOMO),[10c] and the valence electron configuration of Ni(tpy)−CH_3 can be written as $(3d)^8(\pi^*)^1$ rather than $(3d)^9$. This is consistent with the spin density on the Ni atom being close to 0 in the Ni(tpy)−CH_3 species whereas that on the terpyridne ring is close to 1 (see Table 3 (bottom)). The dramatic decrease of the spin density of the terpyridine ring is correlated to the observed increase of charge on the terpyridine ring upon going from the starting materials to **TS3a**.

From the above orbital analysis, we speculate that substitution of the electron donating groups on the tpy ligand may influence its π orbitals and therefore influence the oxidative addition process. The substitution effect on the iodine transfer reaction step was preliminarily examined by changing the tpy ligand to a tri-*tert*-butyl-terpyridine (tpy′) ligand and a transition state structure (**TS3a′**, Figure 5a) analogous to **TS3a** was located. **TS3a′** appears earlier than **TS3a** along the reaction coordinate in terms of the Ni···I and I···$C^{(1)}$ distances. Figure 6 shows that tpy′ lowers the relative energy of **TS3a′** by 1.5 kcal/mol compared to that of **TS3a**. This is consistent with the yield of the coupled product when using the tpy′ ligand is higher than that when using tpy as the ligand.[10c]

3.3. Ni(tpy)−CH_3 Reaction with Isopropyl Iodide. The cross-coupling reactions employing secondary alkyl electrophiles are less frequently reported in the literature compared to those using primary electrophiles.[2c] In this work, isopropyl iodide was used to represent a secondary electrophile, and the resulting coupled product is isobutane. A similar set of reaction steps as those shown earlier in eqs 3a−5a involving an iodine atom transfer, a radical attack, and a reductive elimination can be written as follows:

$$\text{Ni(tpy)}-CH_3 + (CH_3)CHI \rightarrow \text{I}-\text{Ni(tpy)}-CH_3 + (CH_3)_2CH^{\bullet} \quad (3b)$$

$$\text{I}-\text{Ni(tpy)}-CH_3 + (CH_3)CH^{\bullet} \rightarrow CH_3-\text{Ni(tpy)I}-CH(CH_3)_2 \quad (4b)$$

$$CH_3-\text{Ni(tpy)I}-CH(CH_3)_2 \rightarrow \text{Ni(tpy)}-\text{I} + (CH_3)_2CHCH_3 \quad (5b)$$

And the overall reaction equation is:

$$\text{Ni(tpy)}-CH_3 + (CH_{32}CHI \rightarrow \text{Ni(tpy)}-\text{I} + (CH_3)_2CHCH_3 \quad (B)$$

The iodine transfer, the isopropyl radical attack and the reductive elimination steps starting from isopropyl iodide were also examined using B3LYP/BS1 level of theory calculations. Figure 7 gathers the geometries of the reactants, the intermediates, the transition states and the products involved in the reactions of eqs 3b−5b. Figure 8 shows the energy and the free energy profiles for the reactions of eqs 3b−5b. In **TS3b**, the I···Ni distance is 2.792 Å and the I···$C^{(1)}$ distance is 3.187 Å, whereas in **TS3a** these two values are 2.777 and 3.287 Å, respectively. This implies that the iodine atom transfer for isopropyl iodide may be easier than that for propyl iodide. This hypothesis is verified by the energy profile depicted in Figure 8 that shows $\Delta E^{\ddagger}_{3b}$ is 14.9 kcal/mol compared to $\Delta E^{\ddagger}_{3a}$ of 18.0 kcal/mol. The reaction of 3b is uphill by 13.7 kcal/mol in energy compared to 17.2 kcal/mol in the case of the reaction of eq 3a. These data are consistent with the basic organic knowledge that a secondary radical is more stable than a primary radical. For the reaction of eq 4b, the isopropyl radical attacks the Ni atom in I−Ni(tpy)−CH_3, with a transition state at a $C^{(1)}$···Ni distance of 3.009 Å. This process is accompanied by a slight increase of the Ni−I bond length. The oxidative addition product [denoted as Ni(III)-b] is also a six-coordinated Ni(III) complex with a Ni···$C^{(1)}$ distance of 2.012 Å. The radical attack step for Reaction (B) is a bit difficult compared to that for reaction A, in that the free energy of activation for eq 4b is 13.2 kcal/mol, which is higher than that for eq 4a (10.0 kcal/mol). The reductive elimination of Ni(III)-b is achieved by the approach of the two C atoms. The transition state of the reductive elimination is reached at a $C^{(1)}$···$C^{(2)}$ distance of 2.037 Å. The Ni−$C^{(1)}$ and Ni−$C^{(2)}$ bond lengths both increase slightly and the Ni−I bond lengths increase mildly. The free energy profile indicates that the free energy of activation for this step is 19.2 kcal/mol.

The solvation effect (see Table 2) lowers $\Delta G^{\ddagger}$ for the reactions of eqs 3b and 5b by 1.5 and 0.4 kcal/mol, respectively but increases $\Delta G^{\ddagger}_{4b}$ by 0.4 kcal/mol. From the free energy profiles depicted in Figures 4 and 8, and $\Delta G^{\ddagger}$ values collected in Table 2, an interesting feature was found for the cross-coupling reactions employing secondary electrophiles compared to results using primary electrophiles. For the oxidative addition product, Ni(III)-b, there may be two channels: one is the reductive elimination depicted in 5b and the other is the dissociation to a radical which is denoted as eq −4b (e.g., the reverse reaction of 4b). The free energy of activation for the reaction of eq −4b is 16.9 kcal/mol, and that for the reaction of 5b is 19.2 kcal/mol. As both of the reactions of eqs –4b and 5b are first order, the relative reaction rate of these two step can be calculated with $r_{-4b}/r_{5b} = k_{-4b}/k_{5b} = \exp[(G_{TS\_5b} -$

(20) Kohn, W.; Sham, L. J. *Phys. Rev. A* **1965**, *140*, 1133–1138.

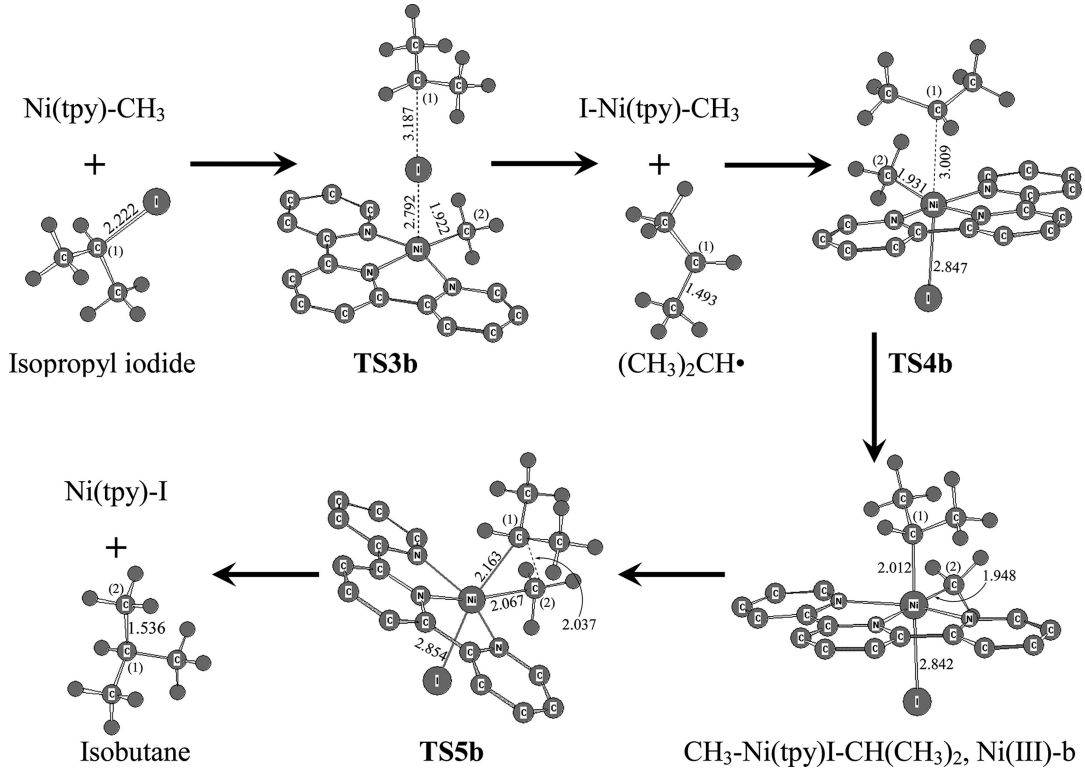

FIGURE 7. Optimized geometries of the reactants, the intermediates, the transition states, and the products involved in the reactions of eqs 3b−5b. Key distances (in Å) are indicated. See the geometries of Ni(tpy)−CH_3, I−Ni(tpy)−CH_3, and Ni(tpy)−I in Figure 3.

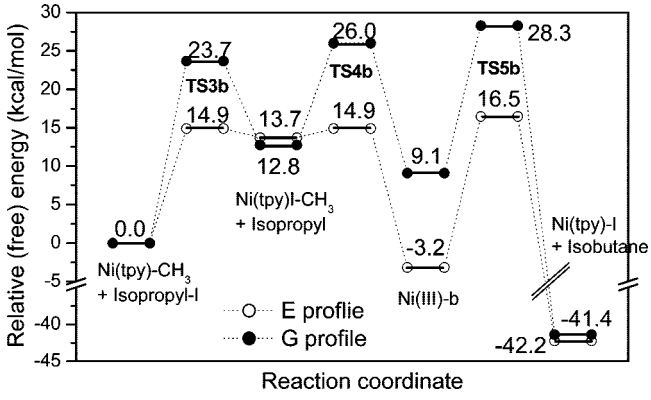

FIGURE 8. Schematic diagram of the energy and the free energy profiles of the reactions of eqs 3b−5b.

$G_{TS\_4b})/RT$], according to the transition state theory,[21] where $G_{TS\_5b} - G_{TS\_4b}$ is the relative free energy of the these two transition states, R the universal gas constant, and T is the temperature. The computed r_{-4b}/r_{5b} is 49 in the gas phase and about 5.6 in the THF solution phase, which shows that the Ni(III)-b species prefers to undergo decomposition *kinetically* and prefers to form the cross-coupling product *thermodynamically*. Because the free radicals are reactive intermediates and the decomposition of the Ni(III)-b species to produce the isopropyl radical increases the risk of side reactions of these radicals may in some cases lead to a noticeably lower yield of the cross-coupling product. The case for reaction B is different from reaction A where k_{5a}/k_{-4a} is about 15 and 67 in the gas and THF solution phases, respectively (see Table 2). This indicates that reaction A is both kinetically and thermodynamically favorable to undergo a reductive elimination over a decomposition reaction. These results may provide a hint for understanding why secondary alkyl electrophiles are less used[2c,9] in the Negishi-tpye cross-coupling reactions than primary ones.

3.4. Transmetalation of Ni(tpy)−I with MeZnI and the Catalytic Cycle. Inspection of reactions A and B shows that both of the reactants and products involve a Ni(I) species. If the Ni(tpy)−I species could react with the transmetalating reagent of R^2ZnX to produce Ni(tpy)−R^2, this process in combination with reactions A and B will form a catalytic cycle. The transmetalation process in this work can be written as:

$$\text{Ni(tpy)}-\text{I} + \text{CH}_3\text{ZnI} \rightarrow \text{Ni(tpy)}-\text{CH}_3 + \text{ZnI}_2 \qquad \text{(C)}$$

And using reaction C with reaction A we get a Negishi reaction:[1,2]

$$\text{CH}_3\text{ZnI} + \text{CH}_3\text{CH}_2\text{CH}_2\text{I} \rightarrow \text{ZnI}_2 + \text{CH}_3\text{CH}_2\text{CH}_2\text{CH}_3 \quad [\text{catalyst: Ni(tpy)}-\text{I or Ni(tpy)}-\text{CH}_3] \qquad \text{(D)}$$

which is the model reaction for reactions depicted in Scheme 1. This catalytic cycle can be described as an oxidative addition, a subsequent reductive elimination that is followed by transmetalation. This description is different from that of the traditional mechanism where the transmetalation step occurs between the oxidative addition and reductive elimination steps. This provides new insight into the Ni-catalyzed Negishi cross-coupling chemistry.

In ref 10c, it was proposed that the Ni(tpy)−I species may undergo transmetalation with an organozinc reagent to form

(21) Kreevoy, M. M.; Truhlar, D. G. In *Investigation of Rates and Mechanism of Reaction*; Techniques of Chemistry, 4th ed., Vol. 6; Bernasconi, C. F., Ed.; John Wiley & Sons: New York, 1986; Part 1, p 13.

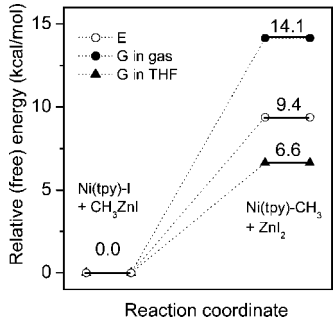

FIGURE 9. Schematic diagram of the energy and the free energy of the Ni(tpy)−CH_3 + ZnI_2 reaction with respect to Ni(tpy)−I + CH_3ZnI in the gas phase and in the solution phase.

Ni(tpy)−R (see Scheme 2) but this has not been experimentally verified. A four-membered-ring transition state in the transmetalation step has been reported for the Pd-catalyzed Suziki cross-coupling reactions[16g,22] and for Stille-reactions.[16e] Despite several attempts, we did not find a four-membered-ring transition state in terms of I the atom transfer from the Ni atom to the Zn atom and the CH_3 transfer from the Zn to Ni atoms in this study. The energy profiles indicate that it is not favorable to produce Ni(tpy)−CH_3 from the Ni(tpy)−I reaction with organozinc reagent, because this needs an energy increase of 9.4 kcal/mol and a free energy increase of 14.1 kcal/mol in the gas phase (see Figure 9). The solvation effect greatly favors the transmetalating products by lowering the free energy change of reaction C by 7.5 kcal/mol. Although the transmetalation step need a mild free energy expense, it is reasonable to expect that reaction C can keep proceeding to the "right" direction, because of the thermodynamic coupling of reactions A or B, which are accompanied by a free energy decrease of 41.9 and 41.4 kcal/mol, respectively. As a catalytic cycle, the free energy change for reaction D is −27.8 kcal/mol.

The results for each of the steps examined in reactions A−C have demonstrated that the reaction mechanism in terms of a catalytic cycle like 3a−5a in conjunction with reaction C is feasible for a Ni(I)-catalyzed Negishi alkyl–alkyl cross-coupling reaction. Figure 10 summarizes the features of such a catalytic process. The oxidative addition process is slightly endothermic, the reductive elimination process is largely exothermic, the transmetalation process is mildly endothermic, and the overall catalytic process is largely exothermic. The oxidative addition occurs in two steps. The first step (e.g., the I atom transfer) is the rate determining step in the oxidative addition and reductive elimination processes.

4. Conclusion

DFT calculations have been used to explore the energy and free energy profiles for Ni-catalyzed Negishi alkyl–alkyl cross-coupling reactions. The poor yield of the cross-coupling product from Ni(II)-propyl iodide in reaction with an organozinc reagent is due to a highly disfavored free energy change of the transmetalation step (eq 1) and not having a large enough

(22) Braga, A. A. C.; Morgon, N. H.; Ujaque, G.; Lledos, A.; Maseras, F. *J. Organomet. Chem.* **2006**, *691*, 4459–4466.

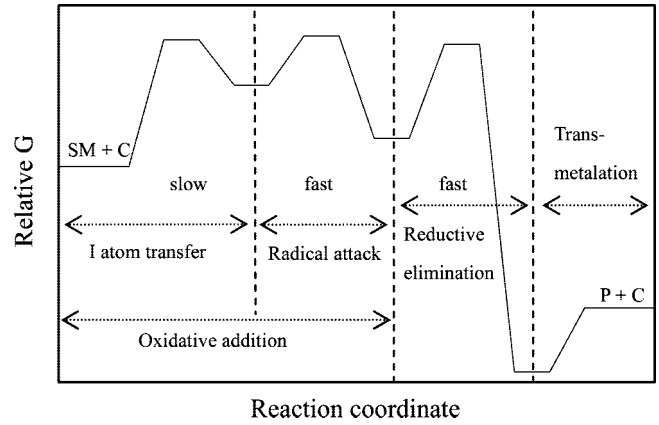

FIGURE 10. Simple schematic diagrams of the full free energy profile for a Ni(I)-catalyzed Negishi alkyl–alkyl cross-coupling reaction. SM is the starting materials including the alkyl halide and organozinc reagent, and P is the products including the cross-coupled and transmetalated products, and C is the catalyst, Ni(tpy)−R.

negative free energy change in the subsequent reductive elimination step (eq 2) for effective thermodynamic coupling. The Ni(I) species (the Ni(tpy)−CH_3 in this study) can react favorably with alkyl iodide to produce a coupled product in terms of the free energy profile and the reaction process involves oxidative addition and reductive elimination. The oxidative addition occurs via a radical pathway involving halogen atom transfer and alkyl radical attack. This reaction mechanism is feasible in terms of the computed free energy of activation and predicted rate constants for each of the steps examined in eqs 3a−5a. The halogen atom transfer step is the rate-determining step and the solvation effect increases the reaction rate of this step. The cross-coupling reaction with secondary alkyl electrophiles was also examined. The rate of the Ni(III) species decomposition is larger than that of its reductive elimination and this may lead to lower yield of the cross-coupled product. Although the transmetalatoin of the Ni(tpy)−I species with CH_3ZnI to form Ni(tpy)−CH_3 is mildly disfavored in terms of the free energy, it may take place due to effective thermodynamic coupling of the Ni(tpy)−CH_3 species reaction with the alkyl halide. Therefore, the catalytic cycle of the Negishi alkyl–alkyl cross-coupling proposed in Scheme 2 is feasible,[10c] and this provides new insights to the chemistry of metal-catalyzed cross-coupling reactions.

Acknowledgment. This research has been supported by grants from the Research Grants Council of Hong Kong (HKU/7021/03P) to D.L.P.

Supporting Information Available: Selected output from the DFT calculations showing the Cartesian coordinates, total energies, vibrational zero-point energies, and free energies (at 298.15 K) for the reactants, intermediates, transition states, and products for the reactions investigated here. The geometry of Ni(tpy′)−CH_3 and selected visualized KS orbitals of Ni(tpy)−CH_3 are included. This material is available free of charge via the Internet at http://pubs.acs.org.

JO702497P